

Current density distribution in the quantum Hall effect

Serkan Sirt¹ and Stefan Ludwig^{1,*}

¹*Paul-Drude-Institut für Festkörperelektronik, Leibniz-Institut im Forschungsverbund Berlin e.V., Hausvogteiplatz 5-7, 10117 Berlin, Germany*

The integer quantum Hall effect (QHE) is one of the most fundamental and important phenomena in condensed matter physics. Its most outstanding application is the resistance standard of the SI units, while new applications are likely to emerge in the advent of quantum technologies. Nevertheless, our microscopic understanding of the QHE is not yet complete. For decades, there has been a controversial discussion about the current density distribution for a quantized Hall resistance. This question is essential for applications as it affects the stability of the quantized Hall states as well as the quantum mechanical phase of the charge carriers. It is also important for the understanding of the fractional, spin or anomalous quantum Hall effects. Here, we discuss the current density distribution based on the screening theory of the QHE. The current flow is chiral and consists of the externally applied imposed and a closed loop persistent current, where the latter decreases as the imposed current is increased.

I. INTRODUCTION

The chirality of trajectories of charged particles exposed to a magnetic field is a fundamental property related with the axial symmetry of the magnetic field vector. In solids, however, boundary conditions and momentum scattering can alter the impact of the axial symmetry and obscure the chirality of trajectories. This is the case for the classical Hall effect, where the Drude model based on momentum scattering predicts a homogeneous unidirectional current density. From this starting point, the question how the Landau quantization, which gives rise to the QHE in a two-dimensional electron system (2DES), changes the current density in a Hall bar is complicated. Albeit, we might argue that the (almost) complete suppression of momentum scattering in the state of quantized Hall resistance should cause the fundamental chirality of trajectories of charged particles to be recovered. Nevertheless, this argument still neglects the influence of the boundaries of the Hall bar. Its edges give rise to a sloped electrostatic potential, which—for the case of a quantized Hall resistance—provides the driving force of dissipationless currents. In equilibrium, a chiral persistent current with density j_{pers} flows [1]. This dissipationless persistent current is a consequence of the non-local nature of the QHE, such that dissipation is moved to the contacts [2, 3].

Applying a voltage between ohmic contacts of the Hall bar breaks the equilibrium and imposes an external current I_{impo} . Recent multiterminal experiments probing the distribution of I_{impo} into various contacts suggest a chiral flow of I_{impo} [4], but no direct local measurements of the current density distribution (including j_{pers}) have been reported for the integer QHE.

The complete local current density inside the Hall bar is $j = j_{\text{pers}} + j_{\text{impo}}$. The imposed current is the integral of the current density over the width of the Hall bar (with its edges at $y = -b$ and $y = b$): $I_{\text{impo}} = \int_{-b}^b dy j = \int_{-b}^b dy j_{\text{impo}}$, while $\int_{-b}^b dy j_{\text{pers}} = 0$, cf. Figures 1 and 2. I_{impo} generates the Hall voltage $V_{\text{H}} = (R_{\text{K}}/\nu)I_{\text{impo}}$, where we introduced the von Klitzing constant $R_{\text{K}} = h/e^2$ and the filling factor ν . The Hall voltage corresponds to the drop of the chemical potential across

the Hall bar, $-eV_{\text{H}} = \int_{-b}^b dy \mu$. Wherever $\mu(y)$ varies, there is a simultaneous change of the energies of all Landau levels (LLs), say $\varepsilon(y)$.

As we will see below, an increase of I_{impo} yields a decrease of $j_{\text{pers}}(y)$. At this point, the non-local nature of the QHE causes a local non-linear current voltage characteristics. In particular, the local dynamics becomes non-Ohmic, meaning that $|j_{\text{impo}}(y)|$ is no longer proportional to $|d\mu/dy|$. Instead, the local density of the dissipationless current is proportional to the energy gradient of the LLs, namely $|j| \propto |d\varepsilon/dy|$, and $j_{\text{impo}}(y) = j - j_{\text{pers}}(y, I_{\text{impo}})$.

Our analysis is based on the electrostatic potential landscape predicted by the screening theory [1, 5–10]. Exposing a 2DES to a high perpendicular magnetic field leads to the collapse of the density of states (DOS) into discrete LLs. Neglecting the Coulomb interaction between charge carriers, the energy gap between LLs would lead to displacements of the electrons causing high local charges. The screening theory goes beyond the scope of the Landauer-Büttiker picture, primarily, by taking into account the direct Coulomb interaction between carriers. This way, it accounts for the tendency of the carriers to minimize the free energy by redistribution (thereby avoiding high local charges) [5]. Nevertheless, in some regions of the 2DES, all LLs end up to be either completely filled or empty. This gives rise to an energy gap ΔE , which (for $k_{\text{B}}T \ll \Delta E$) suppresses any scattering of electrons. Given the lack of accessible unoccupied states, these regions are called incompressible strips (ICSs). The screening theory proposes a fragmentation of the Hall bar in compressible perfectly screened regions, separate by totally unscreened ICSs [8–10]. Inside a compressible region, one LL is partly filled and pinned to the locally constant chemical potential $\mu(y)$. Consequently, inside the unscreened ICSs, $\mu(y)$ varies, while the energy of the LLs changes by ΔE [5].

The early formulations of the screening theory were restricted to the self-consistent solution of the Poisson equation [5] under consideration of the Thomas-Fermi approximation [1]. Later, the screening theory was refined by applying self-consistent non-linear Hartree-type calculation using the Thomas-Fermi approximation and accounting for the quantum mechanical wave properties of the electrons by means of a Gaussian broadening of the LLs [8, 9]. Recently, (for high magnetic fields) the electrostatic results where con-

* ludwig@pdi-berlin.de

firmed within a full self-consistent approach of the quantum-electrostatic problem without using the Thomas-Fermi approximation [11].

Despite its direct connection with the electrostatics, the prediction of the current density distribution for the case of a quantized Hall resistance was until last subject of controversial discussions [1, 5, 10–14], even within the screening theory. Chklovskii et al. calculated the ballistic current through a narrow gate defined channel in the quantum Hall regime by self-consistently solving the Poisson equation using the Thomas-Fermi approximation [1]. They realized, that for a quantized Hall resistance the current flows inside the ICSs. Gerhardt and collaborators used a local version of Ohm's law assuming a dissipative imposed current density $j_{\text{impo}}(y) \propto -d\mu/dy$ to predict j_{impo} based on their refined screening theory [9, 10, 14]. They confirmed that the current flows inside the ICSs. However, they completely neglected j_{pers} [14] and this way predict a non-chiral current flow. Another approach used the continuity equation for predicting j_{impo} [11]. We find this approach questionable, mainly as it considers $I_{\text{impo}} \sim 0$ and, hence, fails to account for the non-linear nature of the problem for reasonable values of I_{impo} .

Our approach differs from the previous attempts to determine j_{impo} . We acknowledge that j_{pers} depends on both, position and I_{impo} , and demonstrate, that a straightforward analysis of the complete current density leads to the prediction of chiral current flow.

Our model follows the simplest possible approach without neglecting j_{pers} . Encouraged by the enormous experimental accuracy of the reproduction of the fundamental von Klitzing constant $R_K = h/e^2$ in QHE measurements [15], we ignore scattering of electrons altogether and consider ballistic transport through ICSs as in Ref. 1. However, we apply this idea to the ICSs predicted by the refined versions of the screening theory [8, 9], which agree with the scanning probe measurements [16–19]. For simplicity, we assume an idealized system at zero temperature, consisting of a perfect 2DES without disorder, and I_{impo} to be much smaller than the break-down current. Further, we neglect any many body correlations, interference effects or details at the interface between compressible regions and the ICSs.

For discussing general properties of the current distribution inside a Hall bar, we restrict ourselves to the first plateau of quantized Hall resistance, where the local filling factor inside the ICSs is $\nu = 1$. We start by sketching in Fig. 1 the predictions of the screening theory [9] for the electrostatic potential distribution across a Hall bar in equilibrium, i.e., for $I_{\text{impo}} = 0$. The Fig. 1(a) contains two ICSs near the edges as expected near the lower magnetic field end of the plateau. In Fig. 1(b) we present a single extended ICS as expected near the higher magnetic field end of the plateau. The upper panels show the variations across the Hall bar of the energy $\varepsilon(y)$ of the first LL as well as the chemical potential $\mu(y)$, which is constant in equilibrium. In the lower panels, we illustrate the fragmentation of the Hall bar in ICSs (dark shaded regions) versus compressible regions (light gray).

The current density is $\vec{j} = -en_s\vec{v}$ with the density n_s and group velocity \vec{v} of the carriers. Inside the ICSs the local

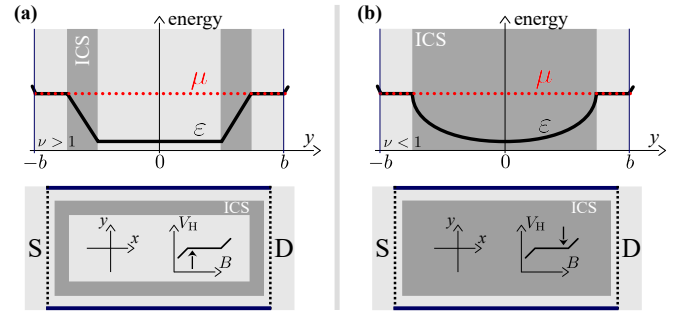


Figure 1. Lower panels: qualitative sketch presenting the fragmentation across the full width of a Hall bar in ICSs (dark shading) and compressible regions (light gray) for equilibrium ($I_{\text{impo}} = 0$), in (a) near the smaller and in (b) near the higher magnetic field end of the plateau, cf. inserts. Upper panels: the red dotted line depicts the chemical potential $\mu(y)$, while the solid line is the energy of the first LL $\varepsilon(y)$ (the confinement potential and other LLs are not shown).

filling factor ν is constant and integer and the carrier density becomes $n_s = \nu n_L$, where n_L is the density per LL (constant and equal for all LLs). For a ballistic electron in an ICS the velocity is $\vec{v} = \vec{E} \times \vec{B}/B^2$, where the driving electric field $\vec{E} = -\nabla\varepsilon/e$ corresponds to the gradient of the LL energy, because the electrons occupy LLs. In our Hall bar geometry with $\vec{E} = -\frac{1}{e}\frac{d}{dy}(0, \varepsilon, 0)$ and $\vec{B} = (0, 0, B)$, (away from the contacts) the current $\vec{j} = (j, 0, 0)$ flows in the $\pm x$ -directions with

$$j = \frac{\nu n_L}{B} \frac{d\varepsilon}{dy} = \frac{\nu}{eR_K} \frac{d\varepsilon}{dy}, \quad (1)$$

where we used $R_K = (\nu B)/(en_s)$. Clearly, inside the compressible regions with $d\varepsilon/dy = 0$ the current density vanishes. On the opposite sides of the Hall bar, $d\varepsilon/dy$ has opposite signs, such that the current flows in opposite directions. Clearly, Eq. (1) predicts a *chiral persistent current* flowing inside ICSs. In equilibrium, $j = j_{\text{pers}}$, which follows a closed loop. In Fig. 2(a) we illustrate the equilibrium behavior for the case of two separate ICSs. We can define the persistent current per ICS to be $I_{\text{pers}} = \int_{\text{ICS}} dy j_{\text{pers}}$. In the bottom plot of Fig. 2(a) I_{pers} corresponds to the regions shaded in blue.

In Fig. 2(b) we sketch a corresponding non-equilibrium situation. Caused by an imposed current, $I_{\text{impo}} \neq 0$, the chemical potential $\mu(y)$ increases monotonously between the edges. Thereby, it varies inside the ICSs but is constant within the perfectly screened compressible regions. This prediction by the screening theory confirmed the results of scanning probe experiments [16–19]. Moreover, various transport experiments confirmed additional aspects of the screening theory [20–26]. All these results contradict the Landauer-Büttiker picture.

In order to apply a useful toy model, we make two additional assumptions: (1) Half of V_H drops in each of the two ICSs, as is the case in the limit $|I_{\text{impo}}| \ll |I_{\text{pers}}|$. (2) The gradient $d\varepsilon/dy$ does not depend on I_{impo} . Although this assumption is inaccurate, it simplifies the illustration, while not influencing the qualitative trend [8–10], namely that the width of the

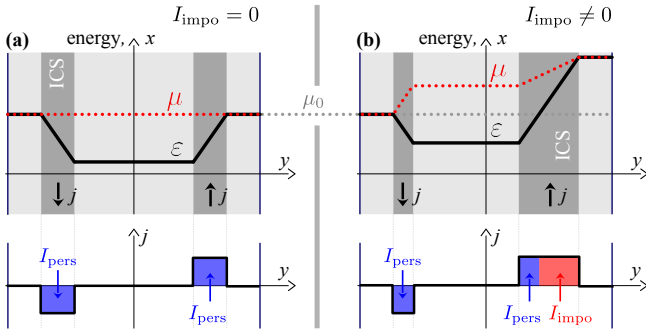


Figure 2. (a) LL energy $\varepsilon(y)$ and chemical potential $\mu(y)$ as in Fig. 1(a) for $I_{\text{impo}} = 0$; current density $j \propto -d\varepsilon/dy$ and resulting I_{pers} (blue areas) flows in opposite directions in the two ICSs at equal magnitude. (b) as in (a) but for $I_{\text{impo}} \neq 0$ assuming unchanged $d\varepsilon/dy$ inside each ICS; the ICS widths, $\varepsilon(y)$ and $\mu(y)$ are altered; $|I_{\text{pers}}|$ is reduced; I_{impo} (red area) flows inside the ICS along the high potential edge of the Hall bar.

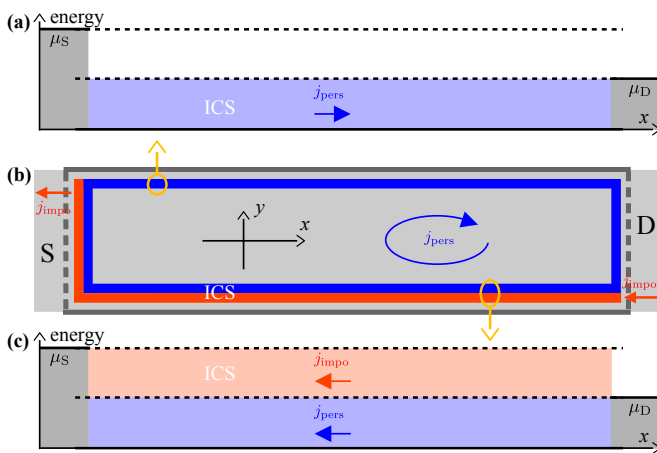


Figure 3. Illustration of geometry in (b) of the ICS corresponding to the non-equilibrium situation with $I_{\text{impo}} \neq 0$ of Fig. 2(b); (a) and (c) are energy diagrams of the ICS along the upper and lower edges, respectively. States contributing to j_{pers} are indicated in blue and those of j_{impo} in red. The persistent current describes a closed path inside the Hall bar as all contributing states have energies below the chemical potentials of both leads, $E < \mu_S, \mu_D$. The imposed current is carried by states with energies $\mu_S \geq E > \mu_D$. Its electrons enter the Hall bar from the source contact, move along its high potential (lower) edge and leave it into empty states of the drain contact.

ICS near the smaller chemical potential is reduced, while the other ICS widens.

The main qualitative result is visible in Fig. 2(b): I_{pers} , which has the identical absolute value on both sides of the Hall bar, is reduced and I_{impo} flows entirely along the high

potential side of the Hall bar.

In Fig. 3, we provide an alternative point of view to refine our analysis. In panel (b), we sketch a minimalistic Hall bar. It consists of two edges connecting the source (S) and drain (D) contacts fixed to the chemical potentials $\mu_S > \mu_D$. The persistent current flows in a closed loop inside the ICS (blue). The imposed current flows through the ICS from drain to source (red). The corresponding electrons moving from source to drain pin the chemical potential of the lower edge to μ_S . Since j_{impo} flows entirely along the lower edge of the Hall bar, its upper edge remains at μ_D . Figures 3 (a) and (c) illustrate the chemical potentials of the contacts and the energy range of the current carrying (occupied) states inside the ICS along the upper versus lower edge, respectively. Shaded regions indicate occupied states (at $T = 0$), gray inside the contacts, blue inside the ICS at energies $E < \mu_D$, and red inside the ICS at energies $\mu_D < E \leq \mu_S$. Electrons with $E \leq \mu_D$ contribute to j_{pers} , electrons with $E > \mu_D$ contribute to j_{impo} . Clearly, j_{pers} follows a closed path inside the Hall bar as for $E \leq \mu_D$ no unoccupied states are available in the leads. In contrast j_{impo} is carried by electrons emitted from the source contact, which then leave the Hall bar into the drain contact, cf. Fig. 3(c). Reflecting the chiral nature of the ICSs, predefined by the local gradients of the LL energies, cf. Fig. 2(b), j_{impo} follows entirely the lower edge.

In summary, by applying the screening theory and considering the complete current density $j = j_{\text{impo}} + j_{\text{pers}}$ inside the Hall bar, we find that the *current flow is chiral* for the case of a quantized resistance. In more detail, we find that, as a consequence of the non-local and non-linear nature of the QHE, the persistent current becomes smaller as the imposed current is increased. While the current flow through the ICSs is chiral, the imposed current flows entirely along the high potential edge of the Hall bar. Although our analysis was focused on the first plateau of the QHE, our findings can easily be generalized and hold for all integer filling factors.

ACKNOWLEDGEMENT

This work was funded by the Deutsche Forschungsgemeinschaft (DFG, German Research Foundation) – 218453298.

CONTRIBUTIONS OF THE AUTHORS

S.L. derived the model and wrote the article. S.S. contributed in many discussions and the production of the figures.

REFERENCES

[1] D. B. Chklovskii, K. A. Matveev, and B. I. Shklovskii, Ballistic conductance of interacting electrons in the quantum Hall

regime, *Phys. Rev. B* **47**, 12605 (1993).

- [2] U. Klauß, W. Dietsche, K. von Klitzing, and K. Ploog, Imaging of the dissipation in quantum-hall-effect experiments, *Zeitschrift für Physik B Condensed Matter* **82**, 351 (1991).
- [3] S. Komiyama, H. Sakuma, K. Ikushima, and K. Hirakawa, Electron temperature of hot spots in quantum hall conductors, *Phys. Rev. B* **73**, 045333 (2006).
- [4] S. Sirt, M. Kamm, V. Y. Umansky, and S. Ludwig, Current distribution and chirality in the regime of the quantized hall effect (2024), [arXiv:2407.01277](https://arxiv.org/abs/2407.01277).
- [5] D. B. Chklovskii, B. I. Shklovskii, and L. I. Glazman, Electrostatics of edge channels, *Phys. Rev. B* **46**, 4026 (1992).
- [6] M. M. Fogler and B. I. Shklovskii, Resistance of a long wire in the quantum Hall regime, *Phys. Rev. B* **50**, 1656 (1994).
- [7] K. Lier and R. R. Gerhardt, Self-consistent calculations of edge channels in laterally confined two-dimensional electron systems, *Phys. Rev. B* **50**, 7757 (1994).
- [8] A. Siddiki and R. R. Gerhardt, Thomas-fermi-poisson theory of screening for laterally confined and unconfined two-dimensional electron systems in strong magnetic fields, *Phys. Rev. B* **68**, 125315 (2003).
- [9] A. Siddiki and R. R. Gerhardt, Incompressible strips in dissipative Hall bars as origin of quantized Hall plateaus, *Phys. Rev. B* **70**, 195335 (2004).
- [10] R. R. Gerhardt, The effect of screening on current distribution and conductance quantisation in narrow quantum Hall systems, *physica status solidi (b)* **245**, 378 (2008), <https://onlinelibrary.wiley.com/doi/pdf/10.1002/pssb.200743344>.
- [11] P. Armagnat and X. Waintal, Reconciling edge states with compressible stripes in a ballistic mesoscopic conductor, *Journal of Physics: Materials* **3**, 02LT01 (2020).
- [12] B. I. Halperin, Quantized hall conductance, current-carrying edge states, and the existence of extended states in a two-dimensional disordered potential, *Phys. Rev. B* **25**, 2185 (1982).
- [13] M. Büttiker, Absence of backscattering in the quantum Hall effect in multiprobe conductors, *Phys. Rev. B* **38**, 9375 (1988).
- [14] K. Güven and R. R. Gerhardt, Self-consistent local equilibrium model for density profile and distribution of dissipative currents in a hall bar under strong magnetic fields, *Phys. Rev. B* **67**, 115327 (2003).
- [15] K. von Klitzing, Developments in the quantum hall effect, *Philosophical Transactions of the Royal Society A: Mathematical, Physical and Engineering Sciences* **363**, 2203 (2005), <https://royalsocietypublishing.org/doi/pdf/10.1098/rsta.2005.1640>.
- [16] K. L. McCormick, M. T. Woodside, M. Huang, M. Wu, P. L. McEuen, C. Duruoz, and J. S. Harris, Scanned potential microscopy of edge and bulk currents in the quantum Hall regime, *Phys. Rev. B* **59**, 4654 (1999).
- [17] P. Weitz, E. Ahlswede, J. Weis, K. Klitzing, and K. Eberl, Hall-potential investigations under quantum Hall conditions using scanning force microscopy, *Physica E: Low-dimensional Systems and Nanostructures* **6**, 247 (2000).
- [18] E. Ahlswede, P. Weitz, J. Weis, K. von Klitzing, and K. Eberl, Hall potential profiles in the quantum Hall regime measured by a scanning force microscope, *Physica B: Condensed Matter* **298**, 562 (2001), international Conference on High Magnetic Fields in Semiconductors.
- [19] E. Ahlswede, J. Weis, K. v. Klitzing, and K. Eberl, Hall potential distribution in the quantum Hall regime in the vicinity of a potential probe contact, *Physica E: Low-dimensional Systems and Nanostructures* **12**, 165–168 (2002), proceedings of the Fourteenth International Conference on the Electronic Properties of Two-Dimensional Systems.
- [20] J. Horas, A. Siddiki, J. Moser, W. Wegscheider, and S. Ludwig, Investigations on unconventional aspects in the quantum hall regime of narrow gate defined channels, *Physica E: Low-dimensional Systems and Nanostructures* **40**, 1130 (2008), 17th International Conference on Electronic Properties of Two-Dimensional Systems.
- [21] A. Siddiki, J. Horas, J. Moser, W. Wegscheider, and S. Ludwig, Interaction-mediated asymmetries of the quantized hall effect, *EPL (Europhysics Letters)* **88**, 17007 (2009).
- [22] A. Siddiki, J. Horas, D. Kupidura, W. Wegscheider, and S. Ludwig, Asymmetric nonlinear response of the quantized hall effect, *New Journal of Physics* **12**, 113011 (2010).
- [23] J. Weis and K. von Klitzing, Metrology and microscopic picture of the integer quantum Hall effect, *Philosophical Transactions of the Royal Society A: Mathematical, Physical and Engineering Sciences* **369**, 3954 (2011), <https://royalsocietypublishing.org/doi/pdf/10.1098/rsta.2011.0198>.
- [24] Kendirlik E. M., Sirt S., Kalkan S. B., Dietsche W., Wegscheider W., Ludwig S., and Siddiki A., Anomalous resistance overshoot in the integer quantum Hall effect, *Scientific Reports* **3**, 3133 (2013).
- [25] E. M. Kendirlik, S. Sirt, S. B. Kalkan, N. Ofek, V. Umansky, and A. Siddiki, The local nature of incompressibility of quantum Hall effect, *Nature Communications* **8**, 14082 (2017).
- [26] S. Sirt, V. Y. Umansky, A. Siddiki, and S. Ludwig, Direct measurement of bulk currents in the quantized hall regime (2024), [arXiv:2405.05138](https://arxiv.org/abs/2405.05138).